

1,2,3,4-Tetraphenyl-1,2,3,4-tetraphospholane, a Highly Versatile Cyclocarbaphosphine Ligand: Reactions with Activated Triosmium Clusters and Characterization of the Products

Siau-Gek Ang,* Xinhua Zhong, and How-Ghee Ang

Department of Chemistry, National University of Singapore, 119260, Singapore

Received March 13, 2002

Reaction of 1,2,3,4-tetraphenyl-1,2,3,4-tetraphospholane (**1**) with $[\text{Os}_3(\text{CO})_{11}(\text{NCMe})]$ at ambient temperature affords substituted clusters: the monosubstituted trinuclear cluster $[\text{Os}_3(\text{CO})_{11}\{\text{(PPh)}_4\text{CH}_2\}]$ (**1**) and the isomeric linked bis-trinuclear clusters $[\{\text{Os}_3(\text{CO})_{11}\}_2\{\mu\text{-}1,4\text{-}\eta^2\text{-}(\text{PPh})_4\text{CH}_2\}]$ (**2**) and $[\{\text{Os}_3(\text{CO})_{11}\}_2\{\mu\text{-}1,3\text{-}\eta^2\text{-}(\text{PPh})_4\text{CH}_2\}]$ (**3**). Clusters **2** and **3** can also be prepared by further reaction of **1** with $[\text{Os}_3(\text{CO})_{11}(\text{NCMe})]$. The reaction at 100 °C gives, apart from cluster **2**, the disubstituted 1,4-bridged trinuclear cluster $[\text{Os}_3(\text{CO})_{10}\{\mu\text{-}1,4\text{-}\eta^2\text{-}(\text{PPh})_4\text{CH}_2\}]$ (**4**). The conversion of **1** into **4** can be achieved through the pyrolysis of a solution of **1**. When **1** reacts with an equimolar amount of $[\text{Os}_3(\text{CO})_{10}(\mu\text{-H})_2]$ at 100 °C in toluene, the 1,2,4-linked bis-trinuclear cluster $[\text{Os}_3(\text{CO})_{11}\{\mu_3\text{-}1,2,4\text{-}\eta^3\text{-}(\text{PPh})_4\text{CH}_2\}\text{-Os}_3(\text{CO})_8(\mu\text{-H})_2]$ (**5**) is obtained. When **1** reacts with a 2-fold molar amount of $[\text{Os}_3(\text{CO})_{10}(\mu\text{-H})_2]$, the 1,2,3,4-linked bis-trinuclear hydride cluster $[\{\text{Os}_3(\text{CO})_8(\mu\text{-H})_2\}_2\{\mu_4\text{-}1,2,3,4\text{-}\eta^4\text{-}(\text{PPh})_4\text{CH}_2\}]$ (**6**) is obtained. Cluster **1** exists as two conformational isomers (**1y** and **1r**) in the crystalline state, due to different conformational arrangements of pseudoaxial carbonyls in the cluster. Cluster **3** shows two interconvertible conformers (**3y** and **3r**) due to the inversion of the configuration of the uncoordinated outer phosphorus atom, and a pair of enantiomers exists in **3r**. All of the new compounds obtained have been characterized by spectroscopic and analytical techniques, and their structures have been established by X-ray crystallography.

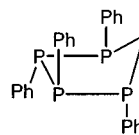
Introduction

The reactions of homocyclopolyposphines $(\text{PR})_n$ ($\text{R} = \text{Ph}, \text{Et}, \text{CF}_3, \text{Bu}^t$; $n = 4, 5$), cyclocarbaphosphines (1,2,3-triphenyl-1,2,3-triphosphaindan,^{3,4} pentaphenyl-1,2,3-triphospholene,⁵ and tetrakis(trifluoromethyl)-1,2-diphosphetene⁶) with iron, ruthenium, and osmium carbonyl clusters

* Author to whom correspondence should be addressed. E-mail: sciangsg@nus.edu.sg. Fax: (65)68723564.

- (1) (a) Ang, H. G.; Koh, L. L.; Zhang, Q. *J. Chem. Soc., Dalton Trans.* **1995**, 2757. (b) Ang, H. G.; Ang, S. G.; Zhang, Q. *J. Chem. Soc., Dalton Trans.* **1996**, 3843. (c) Ang, H. G.; Ang, S. G.; Zhang, Q. *J. Chem. Soc., Dalton Trans.* **1996**, 2773. (d) Ang, H. G.; Ang, S. G.; Kwik, W. L.; Zhang, Q. *J. Organomet. Chem.* **1995**, 485, C10. (e) Ang, H. G.; Ang, S. G.; Zhang, Q. *Phosphorus, Sulfur Silicon Relat. Elem.* **1996**, 110, 145. (f) Ang, H. G.; Aug, K. W.; Ang, S. G.; Rheingold, A. L. *J. Chem. Soc., Dalton Trans.* **1996**, 3131.
- (2) (a) Johnson, B. F. G.; Layer, T. M.; Lewis, J.; Raithby, P. R.; Wong, W. T. *J. Chem. Soc., Dalton Trans.* **1993**, 973. (b) Charalambous, E.; Heuer, L.; Johnson, B. F. G.; Lewis, J.; Li, W. S.; McPartlin, M.; Massey, A. D. *J. Organomet. Chem.* **1994**, 468, C9.
- (3) (a) King, R. B.; Reimann, R. H. *Inorg. Chem.* **1976**, 15, 184. (b) Kyba, E. P.; Hassett, K. L.; Sheikh, B.; Mckennis, J. S.; King, R. B.; Davis, R. E. *Organometallics* **1985**, 4, 994.
- (4) Ang, S. G.; Zhong, X. H.; Ang, H. G. *J. Chem. Soc., Dalton Trans.* **2001**, 1151.
- (5) Ang, H. G.; Ang, S. G.; Wang, X. *J. Chem. Soc., Dalton Trans.* **2000**, 3429.

have been extensively studied in recent years. In most instances, the polyphosphine ligands undergo ring rupture under forcing reaction conditions to afford phosphido- or phosphinidene-substituted cluster derivatives. In cases where the ligand ring frameworks remain intact, the ligands normally act as mono- or bidentate ligands and adopt η^1 or $\mu\text{-}\eta^2$ coordination modes with clusters. Although $(\text{PEt})_5$ has been proposed to act as a tridentate ligand adopting a $\mu_3\text{-}\eta^3$ coordination mode in osmium cluster derivatives, no crystal structures for these clusters have been reported.^{1c} Herein we report the reactions of 1,2,3,4-tetraphenyl-1,2,3,4-tetraphospholane (**1**) with the activated triosmium carbonyl clusters



1,2,3,4-tetraphenyl-1,2,3,4-tetraphospholane, ligand (**1**)

$[\text{Os}_3(\text{CO})_{11}(\text{NCMe})]$ and $[\text{Os}_3(\text{CO})_{10}(\mu\text{-H})_2]$ under various

- (6) Cowley, A. H.; Hill, K. E. *Inorg. Chem.* **1973**, 12, 1446.

conditions, where a series of new cluster derivatives with the ligand ring framework intact are obtained. In these cluster derivatives, **I** is highly versatile in its range of coordination modes, η^1 , μ -1,3- η^2 , μ -1,4- η^2 , μ_3 -1,2,4- η^3 , and μ_4 -1,2,3,4- η^4 , and acts as mono-, bi-, tri-, and tetradentate P-donor ligands in different products, respectively. To the best of our knowledge, very few known ligands have such a variety of coordination modes toward the same metal cluster as observed for the ligand **I**.

Experimental Section

General Procedures. All reactions involving clusters described here were carried out in vacuo using double-tube reaction vessels equipped with Teflon taps. The starting materials $[\text{Os}_3(\text{CO})_{12}]$, $[\text{Os}_3(\text{CO})_{11}(\text{NCMe})]$, $[\text{Os}_3(\text{CO})_{10}(\mu\text{-H})_2]$, and $[(\text{PPh})_4\text{CH}_2]$ were prepared by literature methods.^{7–10} Elemental analysis was carried out at the Microanalytical Laboratory, Department of Chemistry, National University of Singapore. Infrared spectra were recorded as solutions in 1 cm KBr cells on a Bio-Rad FTS-165 spectrometer, ^1H and ^{31}P NMR spectra on Bruker 300 or 500 MHz Fourier transform spectrometers using SiMe_4 (for ^1H) and 85% H_3PO_4 (for ^{31}P) as references, and mass spectra on a Finnigan MAT 95 instrument by the fast atom bombardment technique, using α -nitrobenzyl alcohol or thioglycerol as the matrix solvent.

Reaction of **I with $[\text{Os}_3(\text{CO})_{11}(\text{NCMe})]$.** (a) **At Room Temperature with an Equimolar Ratio.** $[\text{Os}_3(\text{CO})_{11}(\text{NCMe})]$ (150 mg, 0.16 mmol) and **I** (73 mg, 0.16 mmol) were placed in the inner tube of a double-tube reaction vessel and degassed under vacuum. Freshly distilled dichloromethane (10 mL) was placed in the outer tube of the reaction vessel. After degassing with three freeze–pump–thaw cycles, the solvent was then transferred to the inner tube with the reactants. The reaction system was stirred at room temperature overnight. The resultant red solution was evaporated to dryness under reduced pressure. The residue was dissolved in the minimum volume of CH_2Cl_2 and separated by TLC using CH_2Cl_2 –hexane (1:4, v/v) as eluent. One major yellow band of the cluster $[\text{Os}_3(\text{CO})_{11}\{(\text{PPh})_4\text{CH}_2\}]$ (**1**; $R_f = 0.60$, 137 mg, 65%) was eluted and collected. Anal. Found for **1**: C, 32.60; H, 1.66; P, 8.90. Calcd for $\text{C}_{36}\text{H}_{22}\text{O}_{11}\text{Os}_3\text{P}_4$: C, 32.62; H, 1.66; P, 9.35.

(b) **At Room Temperature with a 1:2.5 Molar Ratio.** The reaction conditions were similar to that of (a). $[\text{Os}_3(\text{CO})_{11}(\text{NCMe})]$ (200 mg, 0.22 mmol) reacted with (**I**) (39 mg, 0.09 mmol) in CH_2Cl_2 (10 mL) at room-temperature overnight to afford a red solution and some yellow precipitate. On filtering off the precipitate, the filtrate was analyzed by TLC chromatography using CH_2Cl_2 /hexane (1:3, v/v) as eluent to afford two major bands of cluster $[\{\text{Os}_3(\text{CO})_{11}\}_2\{\mu\text{-1,4-}\eta^2\text{-}(\text{PPh})_4\text{CH}_2\}]$ (**2**; $R_f = 0.57$, 40 mg (together with the precipitate), 21% (based on ligand and the same for **3**), and cluster $[\{\text{Os}_3(\text{CO})_{11}\}_2\{\mu\text{-1,3-}\eta^2\text{-}(\text{PPh})_4\text{CH}_2\}]$ (**3**; $R_f = 0.51$, 73 mg, 38%). The precipitate was identified as the same compound as band 1 from the filtrate. Anal. Found for **2**: C, 25.57; H, 1.29; P, 5.93. Found for **3**: C, 25.63; H, 1.19; P, 5.56. Calcd for $\text{C}_{47}\text{H}_{22}\text{O}_{22}\text{Os}_6\text{P}_4$: C, 25.61; H, 1.00; P, 5.62.

(c) **At 100 °C with Equimolar Amounts.** The reaction conditions were similar to those in (a). $[\text{Os}_3(\text{CO})_{11}(\text{NCMe})]$ (189 mg, 0.20 mmol) reacted with **I** (92 mg, 0.20 mmol) in toluene (10 mL) in a 100 °C oil bath for 4 h. The resulting clear red reaction solution

was evaporated to dryness under reduced pressure. One major compound was obtained from this residue after TLC separation using CH_2Cl_2 /hexane (1:3, v/v) as eluent. This was the yellow cluster $[\text{Os}_3(\text{CO})_{10}\{\mu\text{-1,4-}\eta^2\text{-}(\text{PPh})_4\text{CH}_2\}]$ (**4**; $R_f = 0.57$, 108 mg, 42%). Anal. Found for **4**: C, 32.02; H, 2.02; P, 9.14. Calcd for $\text{C}_{35}\text{H}_{22}\text{O}_{10}\text{Os}_3\text{P}_4$: C, 32.38; H, 1.69; P, 9.56.

(d) **At 100 °C with a 1:2.5 Molar Ratio.** The reaction conditions were similar to those in (c). $[\text{Os}_3(\text{CO})_{11}(\text{NCMe})]$ (200 mg, 0.22 mmol) was treated with **I** (39 mg, 0.09 mmol). Cluster **2** ($R_f = 0.58$, 87 mg, 45%) was obtained after TLC using CH_2Cl_2 /hexane (1/3) as eluent.

Reaction of Cluster **1 with $[\text{Os}_3(\text{CO})_{11}(\text{NCMe})]$.** This reaction was similar to that in (a) above. Cluster **1** (80 mg, 0.06 mmol) was treated with $[\text{Os}_3(\text{CO})_{10}(\text{NCMe})]$ (57 mg, 0.06 mmol) in dichloromethane (10 mL) at room temperature overnight. Clusters **2** ($R_f = 0.56$, 42 mg, 32%) and **3** ($R_f = 0.49$, 58 mg, 45%) were obtained after TLC using CH_2Cl_2 /hexane (1/4) as eluent.

Conversion of Cluster **1 into **4**.** A single reaction vessel was charged with cluster **1** (45 mg, 0.03 mol) in toluene (10 mL). The solution was degassed over three freeze–pump–thaw cycles. The tube and its contents were heated overnight in a 100 °C oil bath. One major band was eluted (CH_2Cl_2 /hexane (1/3)), which was identified by ^{31}P NMR as **4** ($R_f = 0.52$, 28 mg, 74%).

Reaction of Cluster **1 with $[\text{Os}_3(\text{CO})_{10}(\mu\text{-H})_2]$.** This reaction was similar to that in (c). Cluster **1** (60 mg, 0.045 mmol) was treated with $[\text{Os}_3(\text{CO})_{10}(\mu\text{-H})_2]$ (39 mg, 0.045 mmol) in toluene (10 mL) at 100 °C for 4 h. The cluster $[\{\text{H}_2\text{Os}_3(\text{CO})_8\}\{\mu_3\text{-1,2,4-}\eta^4\text{-}(\text{PPh})_4\text{CH}_2\}\{\text{Os}_3(\text{CO})_{11}\}]$ (**5**; $R_f = 0.55$, 36 mg, 38%) was obtained after TLC using CH_2Cl_2 /hexane (3/7) as eluent. Anal. Found for **5**: C, 25.16; H, 1.22; P, 5.31. Calcd for $\text{C}_{44}\text{H}_{24}\text{O}_{19}\text{Os}_6\text{P}_4$: C, 24.88; H, 1.13; P, 5.84.

Reaction of **I with $[\text{Os}_3(\text{CO})_{10}(\mu\text{-H})_2]$.** This reaction was similar to that in (c) above, except that $[\text{Os}_3(\text{CO})_{10}(\mu\text{-H})_2]$ was used instead of $[\text{Os}_3(\text{CO})_{11}(\text{NCMe})]$. $[\text{Os}_3(\text{CO})_{10}(\mu\text{-H})_2]$ (160 mg, 0.19 mmol) was treated with **I** (42 mg, 0.09 mmol) in toluene (10 mL) at 100 °C for 4 h. The cluster $[\{\text{H}_2\text{Os}_3(\text{CO})_8\}_2\{\mu_4\text{-1,2,3,4-}\eta^4\text{-}(\text{PPh})_4\text{CH}_2\}]$ (**6**; $R_f = 0.67$, 54 mg, 28%) was obtained after TLC using CH_2Cl_2 /hexane (3/7) as eluent. Anal. Found for **6**: C, 24.28; H, 1.58; P, 5.57. Calcd for $\text{C}_{41}\text{H}_{26}\text{O}_{16}\text{Os}_6\text{P}_4$: C, 24.14; H, 1.28; P, 6.07.

X-ray Crystallographic Studies. All single crystals for X-ray diffraction analysis were obtained by slow evaporation of a saturated CH_2Cl_2 /hexane solution at -20 °C for several days or by slow diffusion of hexane into dichloromethane solution at -20 °C, unless specially specified. Crystal data and details of the measurement for clusters **1–6** were given in Table 1. Diffraction intensities were collected at 293 K on a Siemens CCD SMART diffractometer using graphite-monochromated Mo K α radiation ($\lambda = 0.71073$ Å) and the ω – 2θ scan technique. The structures were solved by direct methods, and the refinement was by the full-matrix least-squares method with all non-hydrogen atoms refined anisotropically. All computations were carried out using a SHELXTL software package.¹¹

Results and Discussion

Reactions of 1,2,3,4-tetraphenyl-1,2,3,4-tetraphospholane (**I**) with the activated triosmium cluster $[\text{Os}_3(\text{CO})_{11}(\text{NCMe})]$ (Scheme 1) yield the series of mono- and disubstituted cluster derivatives **1–4**. The reaction at room temperature in an equimolar ratio affords the monosubstituted triosmium cluster $[\text{Os}_3(\text{CO})_{11}\{(\text{PPh})_4\text{CH}_2\}]$ (**1**) in 65% yield. In cluster **1**, **I**

(11) Sheldrick, G. M. SHELXTL; Siemens, Madison, WI, 1997.

(7) Johnson, B. F. G.; Lewis, J. *Inorg. Synth.* **1972**, *13*, 93.

(8) Nicholls, J. N.; Vargas, M. D. *Inorg. Synth.* **1989**, *26*, 290.

(9) Kaesz, H. D. *Inorg. Synth.* **1990**, *28*, 238.

(10) Baudler, M.; Vesper, J.; Junkes, P.; Sandmann, H. *Angew. Chem., Int. Ed. Engl.* **1971**, *10*, 940.

Table 1. Summary of Crystallographic Data for Clusters 1–6

	1y	1r	2	3y	3r	4	5	6
formula	C ₃₆ H ₂₂ O ₁₁ - Os ₃ P ₄	C ₃₆ H ₂₂ O ₁₁ - Os ₃ P ₄	C ₄₇ H ₂₂ O ₂₂ - Os ₆ P ₄ ·CH ₂ Cl ₂ · 1/2C ₆ H ₁₄	C ₄₇ H ₂₂ O ₂₂ - Os ₆ P ₄ ·CH ₂ Cl ₂	C ₄₇ H ₂₂ O ₂₂ - Os ₆ P ₄ · 1/2CH ₂ Cl ₂	C ₃₅ H ₂₂ O ₁₀ Os ₃ P ₄ · 1/2CH ₂ Cl ₂	C ₄₄ H ₂₄ O ₁₉ - Os ₆ P ₄	C ₄₁ H ₂₆ O ₁₆ - Os ₆ P ₄ · 1/2CH ₂ Cl ₂
fw	1325.02	1325.02	2331.74	2288.65	2246.19	1339.47	2121.52	2099.38
cryst syst	monoclinic	triclinic	orthorhombic	orthorhombic	monoclinic	monoclinic	monoclinic	monoclinic
space group	C2/c	P1	Ibca	Pna2 ₁	P2 ₁ /n	P2 ₁ /c	P2 ₁ /c	C2/c
a, Å	22.1105(3)	10.01370(10)	13.4535(2)	29.6352(7)	12.2713(2)	19.9501(6)	12.1994(7)	23.0038(3)
b, Å	22.3926(3)	13.3073(2)	24.787 20(10)	16.3231(3)	37.6220(6)	11.4949(3)	22.5939(13)	13.5080(2)
c, Å	15.835 30(10)	15.423(1)	39.05110(10)	12.3117(3)	25.11790(1)	18.1456(5)	18.7303(11)	21.687 00(10)
α, deg		84.2150(10)						
β, deg	101.47(2)	77.5610(10)			96.05(2)	96.0110(10)	94.7990(10)	118.32
γ, deg		89.5250(10)						
V, Å ³	7809.27(16)	1996.59(4)	13022.5(2)	5955.6(2)	11531.5(3)	4138.3(2)	5144.6(5)	5932.18(12)
Z	8	2	8	4	8	4	4	8
λ, Å	0.7107	0.7107	0.7107	0.7107	0.7107	0.7107	0.7107	0.7107
μ (mm ⁻¹)	9.960	9.739	11.913	19.532	13.403	9.397	22.411	26.064
F(000)	4912	1228	8504	4152	8136	2484	3824	7560
no. of rflns collected	34 929	18 573	39 338	38 320	76 277	36 807	41 886	22 161
no. of indep rflns	9847	9586	8347	12 789	28 896	10 387	14 914	7200
R _{int}	0.0431	0.0493	0.0609	0.0715	0.0593	0.1594	0.0553	0.0381
R1 ^a	0.0229	0.0530	0.0458	0.0494	0.0583	0.0670	0.0360	0.0501
wR2 ^b	0.0441	0.1278	0.0854	0.0752	0.1105	0.1185	0.0697	0.1033
S(F ²)	0.982	0.950	1.101	1.037	1.052	0.947	0.923	1.164
T (K)	293(2)	293(2)	293(2)	293(2)	293(2)	293(2)	293(2)	293(2)

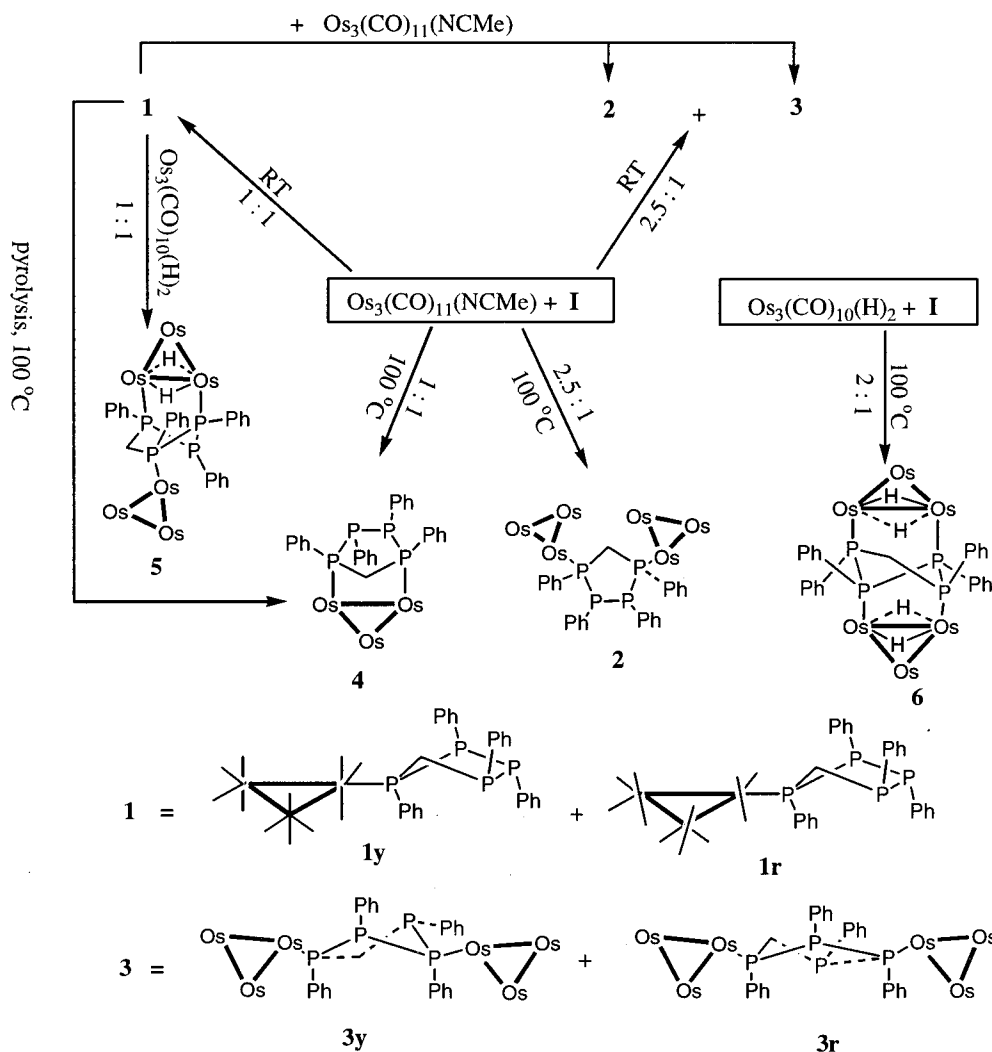
$$^a R1 = \sum(|F_o| - |F_c|) / \sum |F_o|. \quad ^b wR2 = [\sum w(|F_o| - |F_c|)^2 / \sum w(F_o)^2]^{1/2}.$$

shows a η^1 coordination mode, using one of the outer phosphorus atoms to act as a monodentate P-donor. When crystallized in dichloromethane/hexane, **1** presents single crystals of two conformational isomers with different colors (**1y** as yellow and **1r** as red blocks). When the above reaction is performed with a 2.5:1 cluster to ligand ratio, **1** acts as a bidentate donor to give two structurally isomeric linked bis-trinuclear clusters, [$\{\text{Os}_3(\text{CO})_{11}\}_2\{\mu\text{-}1,4\text{-}\eta^2\text{-}(\text{PPh})_4\text{CH}_2\}$] (**2**) and [$\{\text{Os}_3(\text{CO})_{11}\}_2\{\mu\text{-}1,3\text{-}\eta^2\text{-}(\text{PPh})_4\text{CH}_2\}$] (**3**), with good yields (21% and 38%, respectively). **2** and **3** exhibit $\mu\text{-}1,4\text{-}\eta^2$ and $\mu\text{-}1,3\text{-}\eta^2$ coordination modes, respectively. Two configurational isomers (yellow form **3y** and red form **3r**) are isolated for **3** due to the different orientations of the phenyl group on the uncoordinated outer phosphorus atom. A pair of enantiomers is observed in the unit cell of **3r**. When the reaction with equimolar amounts of reactants is carried out at 100 °C, the disubstituted 1,4-bridged cluster [$\text{Os}_3(\text{CO})_{10}\{\mu\text{-}1,4\text{-}\eta^2\text{-}(\text{PPh})_4\text{CH}_2\}$] (**4**) is afforded in 42% yield. In cluster **4**, **1** also shows the $\mu\text{-}1,4\text{-}\eta^2$ coordination mode as seen in **2**. When the reaction is performed with a 2.5:1 cluster to ligand molar ratio at 100 °C, only **2** is obtained. Cluster **1** can undergo further reactions with metal clusters and is the precursor for clusters **2**–**5**. When **1** reacts with an equimolar amount of [$\text{Os}_3(\text{CO})_{11}(\text{NCMe})$] at room temperature, **2** and **3** are obtained in good yields (32% and 45%, respectively). The conversion of **1** into **4** can be achieved in 74% yield through the pyrolysis of the toluene solution of **1** at 100 °C for 4 h. When **1** reacts with an equimolar amount of [$\text{Os}_3(\text{CO})_{10}(\mu\text{-H})_2$] in toluene at 100 °C for 4 h, the 1,2,4-linked bis-trinuclear cluster [$\{(\mu\text{-H})_2\text{Os}_3(\text{CO})_8\}\{\mu_3\text{-}1,2,4\text{-}\eta^3\text{-}(\text{PPh})_4\text{CH}_2\}\{\text{Os}_3(\text{CO})_{11}\}$] (**5**) is formed in 38% yield, wherein ligand **1** acts as a tridentate ligand and shows the $\mu_3\text{-}1,2,4\text{-}\eta^3$ coordination mode. When **1** reacts with a 2-fold molar amount of [$\text{Os}_3(\text{CO})_{10}(\mu\text{-H})_2$] at 100 °C for 4 h, the 1,2,3,4-

linked bis-trinuclear hydride cluster [$\{(\mu\text{-H})_2\text{Os}_3(\text{CO})_8\}_2\{\mu_4\text{-}1,2,3,4\text{-}\eta^4\text{-}(\text{PPh})_4\text{CH}_2\}$] (**6**) is obtained in 28% yield, wherein **1** presents the $\mu_4\text{-}1,2,3,4\text{-}\eta^4$ coordination mode and acts as a tetradentate P donor.

The structures of all of the new clusters obtained have been established by X-ray crystallography and further characterized by IR, FAB mass, and ¹H and ³¹P NMR spectroscopy and elemental analysis (the spectroscopic data are listed in Table 2). Proton-decoupled phosphorus-31 (³¹P{¹H}) NMR spectroscopy is very useful in the elucidation of the structures of the compounds obtained in this study, since the ¹J_{PP} values from directly bonded phosphorus atoms are relatively large (~200 Hz), while the ²J_{PP} and ³J_{PP} values are much smaller and, thus, are readily identifiable from the spectra. For this reason, we have determined that the phosphorus–phosphorus bonds from the ligand moiety in all the clusters obtained remain intact because two of the phosphorus atoms in every cluster have two relatively large ¹J_{PP} coupling constants.

Spectroscopic and Structural Characterization. The Two Conformational Isomers of the Cluster [$\text{Os}_3(\text{CO})_{11}\text{-}\{(\text{PPh})_4\text{CH}_2\}$] (1**).** The carbonyl stretching region of the IR spectrum for cluster **1** (Table 2) is very similar to those of previously reported monosubstituted triosmium cluster derivatives $\text{Os}_3(\text{CO})_{11}(\text{L})$ (L = (PPh)₅,^{1b} (PEt)₅,^{1f} or C₆H₄-(PPh)₃,⁴), which suggests a structural similarity to those species. The ³¹P{¹H} NMR spectrum offers further corroborative evidence to support this proposal. For the signals of two of the phosphorus atoms, we were able to determine two ¹J_{PP} coupling constants (~300 Hz) for each, indicating that the P₄C ring framework of the ligand **1** remains intact in cluster **1**. Of these two signals, the one (at 2.3 ppm) with a smaller ¹J_{PP} coupling constant value (272.9 Hz) is assigned to the coordinated P(1), as the magnitude of the ¹J_{PP} coupling

Scheme 1^a

^a All CO groups on Os atoms are omitted for clarity.

constant is normally reduced when the lone-pair electrons of a tricoordinate phosphorus atom are removed by complexation.¹²

As previously observed for the monosubstituted cluster [Os₃(CO)₁₁{P(p-C₆H₄F)₃}],¹³ cluster **1** has two crystalline forms, a yellow form (**1y**) and a red form (**1r**). Dissolution of **1r** in dichloromethane gives a yellow solution with spectroscopic properties (IR and ¹H and ³¹P NMR spectroscopy) identical with those from the solution of **1y**. When a solution of **1y** or **1r** is recrystallized, both crystalline forms are also obtained.

The structures of both the yellow form (**1y**) and the red form (**1r**) of the cluster **1** have been determined by X-ray diffraction analysis. The molecular structures of **1y** and **1r** are shown in Figure 1 together with the atomic labeling schemes. Selected bond lengths and angles are given in Table 3. The structure of **1y** has the typical structure for the monosubstituted tricosmium cluster [Os₃(CO)₁₁(PR₃)] (PR₃ =

phosphine, phosphite),^{1,4,5,14–20} where the geometry is approximately based on the *D*_{3h} form of [Os₃(CO)₁₂] with one of the equatorial carbonyls replaced by the ligand and all the axial carbonyls nearly perpendicular to the tricosmium plane. The range of the Os–Os bond lengths in cluster **1y** is 2.8869(2)–2.9102(2) Å. The small difference (about 0.023 Å) in the Os–Os separations in **1y** demonstrates that the cone angle of the ligand **I** is not large. The P₄C ring of the ligand moiety has an envelope conformation with P(2), P(3), P(4), and C(1) almost coplanar with a deviation of 0.06 Å,

(12) Jameson, C. J. In *Phosphorus-31 NMR Spectroscopy in Stereochemical Analysis: Theoretical Considerations: Spin–Spin Coupling*; Verkade, J. G., Quinn, L. D., Eds.; VCH: New York, 1987; Chapter 6.

(13) Hansen, V. M.; Ma, A. K.; Biradha, K.; Pomeroy, R. K.; Zaworotko, M. J. *J. Organometallics* **1998**, *17*, 5267.

(14) Benfield, R. E.; Johnson, B. F. G.; Raithby, P. R.; Sheldrick, G. M. *Acta Crystallogr.* **1978**, *B34*, 666.

(15) Ehrenreich, W.; Herberhold, M.; Suss-Fink, G.; Klein, H.-P.; Thewalt, U. *J. Organomet. Chem.* **1983**, *248*, 171.

(16) Suss-Fink, G.; Pellinghelli, M. A.; Tiripicchio, A. *J. Organomet. Chem.* **1987**, *320*, 101.

(17) Bruce, M. I.; Liddell, M. J.; Hughes, C. A.; Skelton, B. W.; White, A. H. *J. Organomet. Chem.* **1988**, *347*, 157.

(18) Heuer, L.; Schomburg, D. *J. Organomet. Chem.* **1995**, *495*, 53.

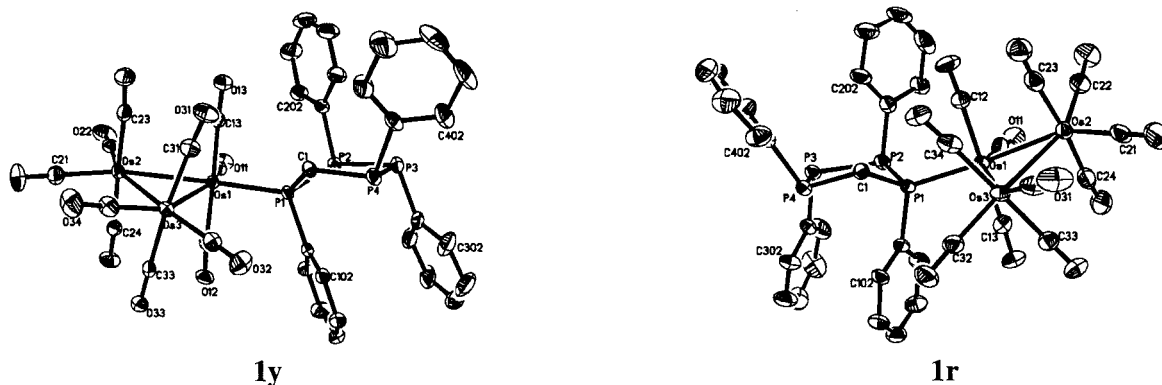
(19) Johnson, B. F. G.; Lewis, J.; Nordlander, E.; Raithby, P. R. *J. Chem. Soc., Dalton Trans.* **1996**, 3825.

(20) (a) Ang, H. G.; Kwik, W. L.; Leong, W. K.; Potenza, J. A. *Acta Crystallogr.* **1989**, *C45*, 1713. (b) Ang, H. G.; Cai, Y. M.; Kwik, W. L.; Leong, W. K.; Tocher, D. A. *Polyhedron* **1991**, *10*, 881. (c) Ang, H. G.; Cai, Y. M.; Kwik, W. L. *J. Organomet. Chem.* **1993**, *448*, 219.

Table 2. Spectroscopic Data for Clusters **1**–**6**

complex	IR $\nu(\text{CO})$, ^a cm^{-1}	¹ H NMR, δ (J, Hz) ^b	³¹ P{ ¹ H} NMR, δ (J, Hz) ^b	MS, m/z ^c
1	2105 m, 2052 s, 2035 m, 2018 vs, 1999 w, 1986 m, 1970 w	6.9–7.7 (m, 20H, Ph) 3.9 (m, 1H, CH ₂) 3.2 (m, 1H, CH ₂)	20.0 (ddd, 288.1, 19.1, 5.0, P ⁴) 5.9 (ddd, 307.3, 288.1, 8.1, P ³) 2.3 (ddd, 272.9, 19.2, 8.1, P ¹) –2.2 (ddd, 307.3, 272.9, 5.0, P ²)	1325 (1325)
2	2107 m, 2057 s, 2035 w, 2023 vs, 1990 w, 1968 w	7.1–7.6 (m, 20H, Ph) 3.8 (m, 2H, CH ₂)	AA'XX' spin pattern δ_A –19.4, δ_X –28.1 $J_{XX'} = 6.7$, $J_{AA'} = 192.2$ $J_{AX} = 262.7$, $J_{AX'} = 14.0$	2204 (2204)
3r	2106 m, 2057 s, 2036 w, 2023 vs, 1989 w, 1968 w	6.7–8.0 (m, 20H, Ph) 3.7 (m, 1H, CH ₂) 3.2 (m, 1H, CH ₂)	14.6 (ddd, 305.0, 15.8, 5.5, 1P) 5.8 (m, 1P) 3.8 (m, 1P) –7.8 (305.0, 269.2, 61.6, 1P))	2204 (2204)
3y	2106 m, 2057 s, 2036 w, 2023 vs, 1989 w, 1968 w	6.7–8.0 (m, 20H, Ph) 3.7 (m, 1H, CH ₂) 3.2 (m, 1H, CH ₂)	4.2 (ddd, 339.4, 79.0, 4.5, P ¹ or P ⁴) –0.5 (ddd, 290.2, 275.8, 4.5, P ² or P ³) –20.2 (ddd, 275.8, 79.0, 20.3, P ¹ or P ⁴) –27.6 (ddd, 339.4, 290.2, 20.3, P ² or P ³)	2204 (2204)
4	2094 s, 2035 w, 2017 s, 2008 vs, 1976 w	6.7–8.2 (m, 20H, Ph) 3.6 (m, 2H, CH ₂)	8.9 (ddd, 232.7, 206.0, 18.0, P ² or P ³) –20.3 (dd, 293.8, 232.7, P ² or P ³) –28.8 (ddd, 293.7, 72.5, 18.0, P ¹ or P ⁴) –34.3 (206.0, 72.5, P ¹ or P ⁴)	1297 (1297)
5	2110 m, 2074 m, 2059 m, 2022 vs, 2007 s, 1995 s, 1951 w	6.7–8.3 (m, 20H, Ph) 4.1 (m, 1H, CH ₂) 3.6 (m, 1H, CH ₂) –10.5 (m, 1H, M–H) –10.8 (m, 1H, M–H)	32.0 (ddd, 201.8, 143.5, 73.4, P ²) 4.6 (ddd, 169.9, 73.4, 20.1, P ⁴) –4.2 (ddd, 201.8, 169.9, 58.5, P ³) –12.2 (ddd, 143.5, 58.5, 20.1, P ¹)	2121 (2121)
6	2083 w, 2069 s, 2049 w, 2013 vs, 1995 w, 1956 w	7.2–8.0 (m, 20H, Ph) 3.9 (m, 2H, CH ₂) –10.6 (d, 2H, M–H) –11.0 (d, 2H, M–H)	AA'BB' spin pattern δ_A 17.0, δ_B –1.1 $J_{AA'} = 206.5$, $J_{XX'} = 0$; $J_{AX} = 145.7$, $J_{AX'} = 28.8$	2040 (2040)

^a In CH₂Cl₂. ^b In CDCl₃ with SiMe₄ for ¹H and 85% H₃PO₄ for ³¹P as references. ^c Simulated values given in parentheses.

**Figure 1.** ORTEP drawings (thermal ellipsoid 30% probability) of clusters **1y** and **1r**.**Table 3.** Selected Bond Lengths (Å) and Angles (deg) for Clusters **1** and **4**

	1y	1r	4
Os(1)–Os(2)	2.8928(2)	2.8672(5)	2.8934(8)
Os(2)–Os(3)	2.8869(2)	2.8724(5)	2.8794(9)
Os(3)–Os(1)	2.9102(2)	2.9090(5)	2.8888(8)
Os(1)–P(1)/ Os(3)–P(4)	2.3472(9)	2.342(2)	2.343(4)/ 2.344(4)
P–P (range)	2.205(2)– 2.239(2)	2.198(3)– 2.217(3)	2.223(5)– 2.276(6)
Os–Os–Os (range)	59.665(5)– 60.467(5)	59.46(2)– 60.91(2)	59.73(2)– 60.21(2)
P–Os–Os (range)	100.66(2)	106.17(5)	87.4(1)– 91.80(9)

and the coordinated phosphorus atom P(1) is out of the above plane at a distance of 0.12 Å. The phenyl groups attached to the neighboring phosphorus atoms adopt an all-trans configuration, which is similar to that in the free ligand.²¹

The most significant difference in the structures of **1r** and **1y** is the orientation of the axial carbonyls. In **1r**, the pseudoaxial carbonyls are severely twisted with respect to each other. The extent of this twisting is measured by the absolute value of the dihedral angle between the averaged planes C_{ax}–Os(2)–C_{ax}–Os(3) and C_{ax}–Os(3)–C_{ax}–Os(2) of the Os₂(CO)₈ fragment of the clusters. In **1r** this dihedral angle (i.e., that between the C(23)Os(2)C(24)Os(3) and C(34)Os(3)C(33)Os(2) planes) is 27.7°. The corresponding angle for **1y** is 13.0°. The Os–Os distances in **1r** (ranging from 2.8672(5) to 2.9090(5) Å) are shortened compared to the corresponding distances in **1y**. These shorter bond lengths suggest that the metal–metal bonds in **1r** are somewhat stronger than those in **1y**, which is in contrast to the observation for the yellow and red forms of [Os₃(CO)₁₁{P(*p*-C₆H₄F)₃}]¹³ and contrary to the view that in the staggered form of M₃(CO)₁₂ there is less metal–metal bonding than in the eclipsed form.²²

(21) Lex, V. J.; Baudler, M. Z. *Anorg. Allg. Chem.* **1977**, 431, 49.

Table 4. Selected Bond Lengths (Å) and Angles (deg) for Clusters **2**, **3**, **5**, and **6**

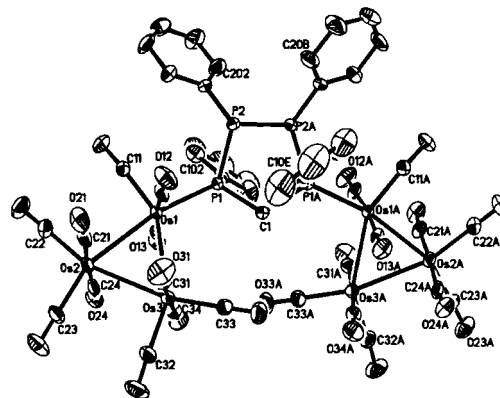
	2 ^a	3y	3r ^b	5	6 ^c
Os(1)–Os(2)	2.8775(4)	2.8630(8)	2.8778(6), 2.8818(6)	2.8645(4)	2.6823(6)
Os(2)–Os(3)	2.8941(5)	2.8755(9)	2.8738(7), 2.8624(6)	2.8710(4)	2.8168(6)
Os(3)–Os(1)	2.9182(4)	2.9062(8)	2.9098(7), 2.8814(7)	2.8887(4)	2.7992(6)
Os(4)–Os(5)		2.8741(8)	2.8707(7), 2.8663(7)	2.6696(3)	
Os(5)–Os(6)		2.8777(8)	2.8610(7), 2.8642(6)	2.7883(4)	
Os(6)–Os(4)		2.9103(8)	2.9186(7), 2.9116(7)	2.8130(4)	
Os–P (range)	2.341(2)	2.345(3)–2.351(4)	2.327(3)–2.367(3)	2.337(2)–2.339(2)	2.315(2)–2.332(3)
P–P (range)	2.212(4)–2.232(3)	2.226(5)–2.250(5)	2.199(4)–2.279(4)	2.230(2)–2.289(2)	2.261(5)–2.263(4)
Os–Os–Os (range)	59.35(2)–60.74(2)	59.36(2)–60.85(2)	59.23(2)–61.22(2)	56.926(8)–62.00(2)	57.06(2)–61.80(2)
P–P–P (range)	90.22(9)	94.1(2)–98.2(2)	97.9(2)–102.6(2)	86.51(8)–91.05(8)	86.9(2)
P–Os–Os (range)	108.77(6)	100.5(1)–101.55(9)	98.65(7)–111.19(7)	94.67(4)–111.38(4)	94.65(6)–95.74(6)

^a A 2-fold axis passes through C(1) and the midpoint of P(2)–P(2A); the two parts of the molecule are equal. ^b Two molecules exist in the unit cell. ^c A 2-fold axis passes through C(1) and the midpoint of P(1)–P(1A); the two parts of the molecule are equal.

The origin of the staggered configuration of the red isomer of **1** may be the same as that for the cluster Os₃(CO)₁₁[P(*p*-C₆H₄F)₃].¹³ As discussed before, the cone angle of ligand **I** is not large; hence, unlike the case for the ligand P(Bu)^t,¹³ which has a large cone angle, steric effects cannot be the cause of this twisting. In comparison with the other cyclopolyphosphines, which we have previously studied, **I** has no extraordinary σ -donor or π -acceptor properties; therefore, the twisting of **1r** looks unlikely to be due to any unusual electronic properties of **I**. Spectroscopic results (IR and ¹H and ³¹P NMR spectra) show that both **1y** and **1r** have identical properties in the solution state. This suggests that intermolecular interactions in the solid state may cause the twisting in **1r**.

Structural Isomers [{Os₃(CO)₁₁]₂{ μ -1,4- η^2 -(PPh)₄CH₂}] (**2**) and [{Os₃(CO)₁₁]₂{ μ -1,3- η^2 -(PPh)₄CH₂}] (**3**). The IR spectra of clusters **2** and **3** are very similar to those of previously reported linked bis-trinuclear clusters [{(Os₃(CO)₁₁)]₂{ μ - η^2 -(L)}].^{1b,4,5,23} As in the free ligand,²⁴ the ³¹P{¹H} NMR spectrum of cluster **2** shows a typical AA'XX' second-order spin pattern, from which we can calculate $J_{AA'}$ = 192.2 Hz, $J_{XX'}$ = 6.7 Hz, J_{AX} = 262.7 Hz, and $J_{AX'}$ = 14.0 Hz.²⁵ Of the two possible modes of coordination (i.e. two triosmium triangles coordinating with either the two outer phosphorus atoms or the two central phosphorus atoms) X-ray crystallographic results confirm the coordination via the outer phosphorus atoms.

The molecular structure of **2** is depicted in Figure 2 together with the atomic labeling scheme, and selected structural parameters are listed in Table 4. A crystallographic 2-fold axis passes through C(1) and the midpoint of the P(2)–P(2A) bond relating the two equal halves of the molecule. In the molecule, ligand **I** links two different triosmium triangles via the equatorial positions using two symmetrical outer phosphorus atoms P(1) and P(1A) and adopting a μ -1,4- η^2 coordination mode. Unlike the all-trans configuration in the free ligand, in the ligand moiety of cluster **2**, Ph² adopts a cis configuration with respect to

**Figure 2.** ORTEP drawing (thermal ellipsoid 30% probability) of cluster **2**.

neighboring Ph¹. This results in a severely distorted P₄C ring framework with P(1) and P(1A) symmetrically located on opposite sides of the plane C(1)P(2)P(2A) at a distance of 0.378 Å. Unlike the 1,3-linked cluster **3** discussed below, the 1,4-linked cluster **2** has low solubility in most common solvents, which may be due to its higher symmetry.

When pure cluster **3** is crystallized in CH₂Cl₂/hexane (1:4), crystals of two colors (red, **3r**; yellow, **3y**) are obtained. The ³¹P{¹H} NMR spectrum of a freshly prepared solution of **3r** in CDCl₃ shows two sets of signals with four phosphorus resonances each. The integration intensity ratio of the two sets is 2.4:1. When the spectrum of **3y** is recorded under the same conditions, the same pattern of signals is obtained but with different relative intensities (1.1:1). This demonstrates that the pure compound **3r** in the solid state can partly convert to **3y** in the solution state and vice versa. The conversion rate is slow compared to the NMR time scale even at elevated temperature (80 °C) in *d*₈-toluene solution. At room temperature, a solution of **3r** in CDCl₃ takes 32 h to establish the equilibrium with a final intensity ratio of 1.6:1, while **3y** requires 26 h to reach equilibrium with the same intensity ratio. It is reasonable to assign the set of signals with greater intensities to **3r** and the other to **3y**. In **3y**, the P(1) and P(4) atoms have an unusually large coupling (²J_{PP} = 79.0 Hz), which may be attributed to their proximity (the nonbonding distance between the two atoms is 3.07 Å).

The structures of both **3r** and **3y** have been determined by X-ray diffraction and are shown in Figure 3, together with the atomic numbering scheme. Selected important bond

(22) Lauher, J. W. *J. Am. Chem. Soc.* **1986**, *108*, 1521.(23) Amoroso, A. J.; Johnson, B. F. G.; Lewis, J.; Massey, A. D.; Raithby, P. R.; Wong, W. T. *J. Organomet. Chem.* **1992**, *440*, 219.(24) Hoffman, P. R.; Caulton, K. G. *Inorg. Chem.* **1975**, *14*, 1997.(25) Sohar, P. In *Nuclear Magnetic Resonance Spectroscopy*; CRC Press: Boca Raton, FL, 1983; Vol. 1, Chapter 1.

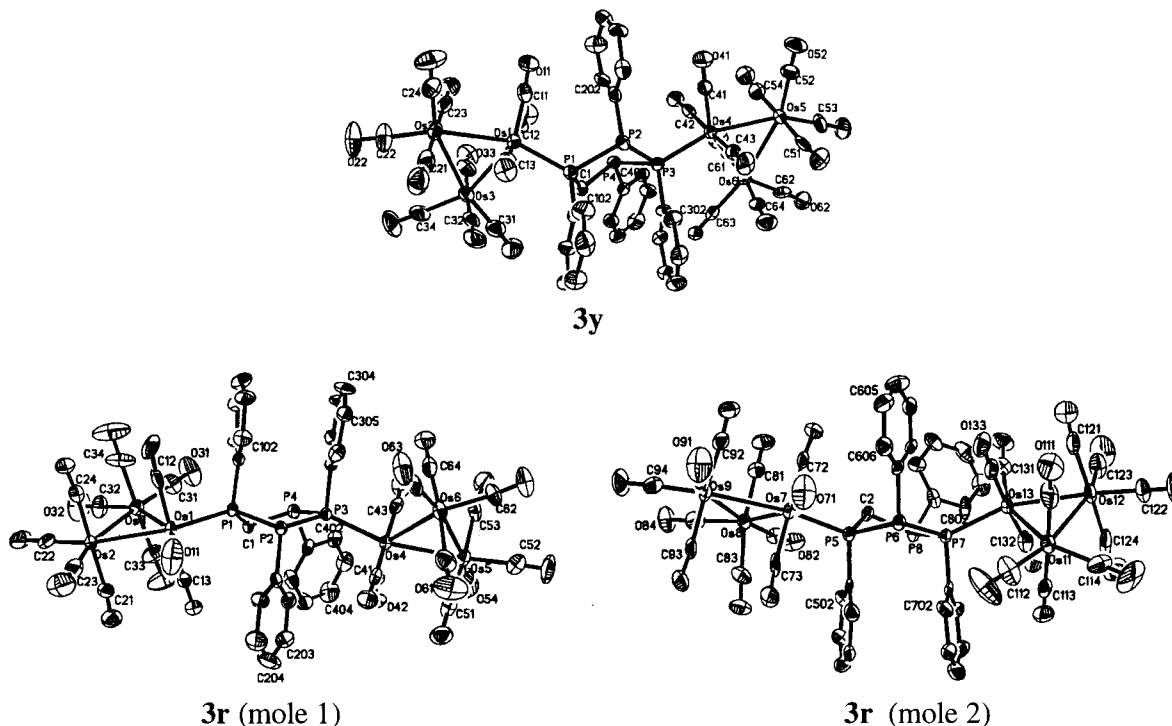
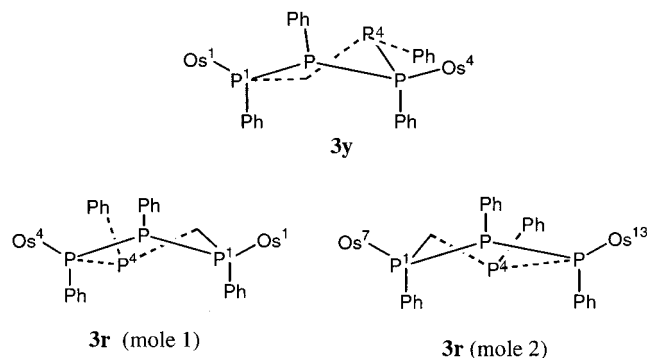


Figure 3. ORTEP drawings (thermal ellipsoid 30% probability) of clusters **3y** and **3r**.

Chart 1. Schematic Structure of Cluster **3**



parameters for both molecules are listed in Table 4. Clusters **3** and **2** are structural isomers. Unlike the case in the free ligand, the phenyl group on the uncoordinated outer phosphorus atom (Ph^4) has a cis configuration with respect to the neighboring Ph^3 , which results in a twisted configuration of the P_4C ring with C(1) and P(4) on opposite sides of the plane P(1)P(2)P(3) at distances of 0.09 and 0.31 Å, respectively.

There are two independent molecules, which are a pair of enantiomers, in the unit cell of **3r**. At the same time, clusters **3r** and **3y** are convertible configurational isomers. The structures of **3r** and **3y** differ essentially in the orientations of the Ph^4 group (Chart 1). Unlike **3y** and just like the free ligand, Ph^4 in **3r** has a trans configuration with respect to the neighboring phenyl (Ph^3). Obviously, the steric crowding among phenyl groups is more pronounced in isomer **3y** than that in **3r**, as shown by the distortion of the P_4C rings. In **3y** this overcrowding is partly or totally compensated by the lesser repulsion between Ph^4 and the $\text{Os}(\text{CO})_3$ unit, with the Ph^4 group pointing away from the $\text{Os}(\text{CO})_3$ unit. This kind of isomeric relationship has been previously reported.^{1c,5}

The P_4C ring of the ligand in **3r** has an envelope configuration, with C(1), P(2), P(3), and P(4) almost coplanar (with a deviation of 0.04 Å) and P(1) out of the plane at a distance of 0.15 Å. The conformations of the axial carbonyl groups of the two discrete trisodium triangles in **3r** are different. In the Os(1)–Os(2)–Os(3) triangle, the axial carbonyl groups give an eclipsed configuration with a dihedral angle of 4.2° between C(24)Os(2)Os(3)C(21) and C(34)Os(3)Os(2)C(33), while in the Os(4)Os(5)Os(6) triangle, the pseudoaxial carbonyl groups are severely twisted. The dihedral angle between C(64)Os(6)Os(5)C(61) and C(53)Os(5)Os(6)C(51) is 23.6°.

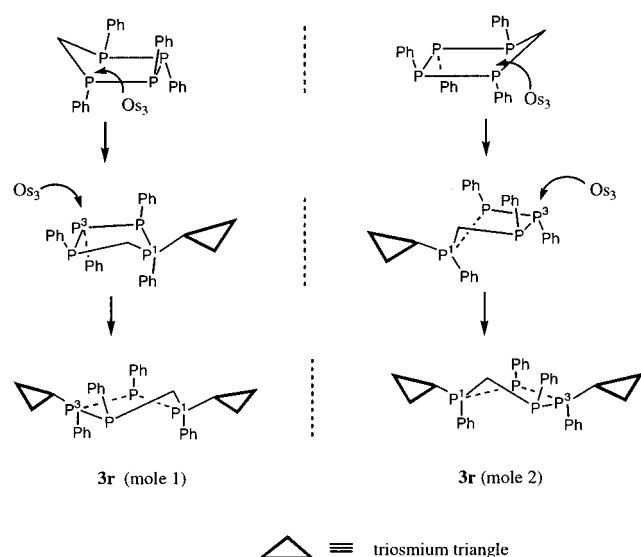
The two coordinated phosphorus atoms in cluster **3** are both chiral atoms; thus, theoretically as many as four diastereomers could be present in both **3y** and **3r**. For the free ligand in the solution state, the phenyl groups on the phosphorus atoms in the P_4C ring adopt an all-trans configuration, which has been confirmed by NMR spectroscopy;²⁴ thus, the free ligand has a pair of enantiomers in the solution state. As shown in Scheme 2, the enantiomeric pair in ligand **I** gives rise to a pair of enantiomers of the monosubstituted cluster **1**, which is confirmed by the X-ray structure. It follows then that the enantiomeric pair of cluster **1** gives rise to a pair of enantiomers in **3r**. Similarly, there should also be a pair of enantiomers in **3y**.

The Cluster $[\text{Os}_3(\text{CO})_{10}\{\mu\text{-}1,4\text{-}\eta^2\text{-}(\text{PPh})_4\text{CH}_2\}]$ (**4**). The IR spectrum (carbonyl stretching region) of cluster **4** shows a vibrational pattern similar to that for previously reported bridged trinuclear clusters $[\text{Os}_3(\text{CO})_{10}\{\mu\text{-}2\text{-}\eta^2\text{-}(\text{L})\}]$.^{1b,4,5,26–28} The NMR spectra clearly indicate that the P_4C ring frame-

(26) Clucas, J. A.; Dawson, R. H.; Dolby, P. A.; Harding, M. M.; Pearson, K.; Smith, A. K. *J. Organomet. Chem.* **1986**, *311*, 153.

(27) Deeming, A. J.; Donovan-Mtunzi, S.; Hardcastle, K. I.; Kabir, S. E.; Henrick, K.; McPartlin, M. *J. Chem. Soc., Dalton Trans.* **1988**, 579.

Scheme 2



work of ligand **I** remains intact in the cluster. The molecular structure of cluster **4** is given in Figure 4 together with the atomic labeling scheme, and the important bond lengths and angles are listed in Table 3. In the cluster, ligand **I** acts as a bidentate donor, occupying equatorial sites on the osmium triangle plane and bridging over an Os–Os edge through the two outer phosphorus atoms P(1) and P(4), adopting a μ -1,4- η^2 coordination mode. Unlike the monosubstituted triosmium cluster derivatives, the three Os–Os edges are not very different in length (ranging from 2.8794(9) to 2.8934(8) Å). The bridged edge Os(1)–Os(3) is not the longest Os–Os separation, which is in contrast to the observations in previously reported bridged triosmium clusters $[\text{Os}_3(\text{CO})_{10}\{\mu\text{-}\eta^2\text{-L}\}]$ (where L = PhP(CH₂)_nPPh, $n = 2\text{--}4$).^{27,28} The P₄C ring of the ligand has a twisted configuration with P(1) and C(1) atoms nearly symmetrically located on opposite sides of the P(2)P(3)P(4) plane at distances of 0.133 and 0.170 Å, respectively. Unlike the free ligand, Ph⁴ adopts a cis configuration with respect to the neighboring Ph³. To accommodate the relatively short Os–Os edge distance, the angle P(1)–C(5)–P(4) (102.1(6)°) is significantly smaller than that in the free ligand (116.62(77)°).²¹ Among the nonbonding P \cdots P distances, P(1) \cdots P(4) is exceptionally short (2.895 Å), while the other two distances are 3.294 and 3.426 Å, respectively. This short distance can explain why $^2J_{\text{P}(1)\text{--}\text{P}(4)}$ is extraordinarily large (72.5 Hz).

The Cluster $[\text{Os}_3(\text{CO})_{11}\{\mu_3\text{-}1,2,4\text{-}\eta^3\text{-}(\text{PPh})_4\text{CH}_2\}\text{Os}_3\text{-}(\text{CO})_8(\mu\text{-H})_2]$ (**5**). The $^{31}\text{P}\{^1\text{H}\}$ NMR spectrum of **5** shows an almost perfect first-order pattern with four resonance signals of equal intensity. All the $^1J_{\text{PP}}$ coupling constants are unusually small, possibly due to the high degree of complexation of the trivalent phosphorus atoms. We assign the smallest $^1J_{\text{PP}}$ value (143.5 Hz) to the coupling between the two coordinated phosphorus atoms P(1) and P(2) with the aid of the X-ray structure. The ^1H NMR spectrum also

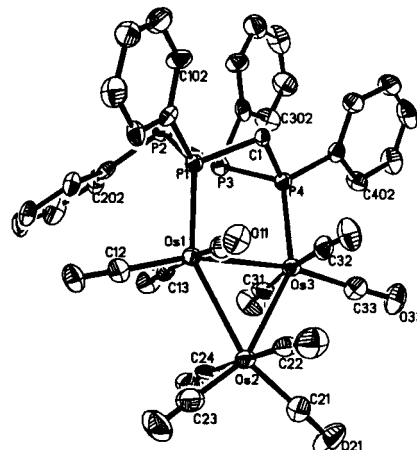


Figure 4. ORTEP drawing (thermal ellipsoid 30% probability) of cluster **4**.

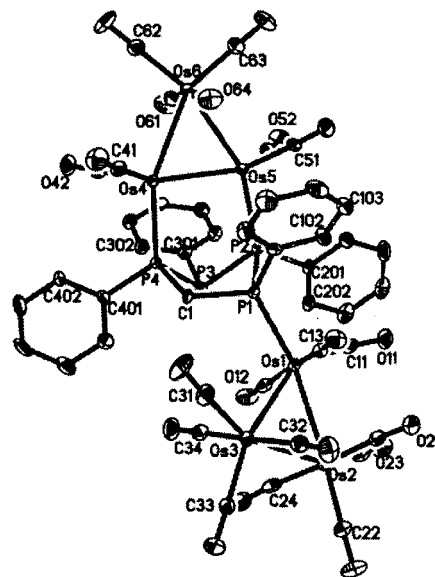


Figure 5. ORTEP drawing (thermal ellipsoid 30% probability) of cluster **5**.

clearly indicates the existence of two metal hydrides (δ at -10.4 and -10.8 ppm, respectively) in the cluster.

Suitable red single crystals of **5** for X-ray crystallography are obtained via the slow evaporation of a saturated chloroform solution at ambient temperature. The molecular structure is given in Figure 5 together with the atomic labeling scheme, and selected bond parameters are listed in Table 4. The cluster **5** can be considered as an extension of the monosubstituted cluster **1** with the two other phosphorus atoms (P(2) and P(4)) in the ligand moiety coordinating with another triosmium triangle via the displacement of two carbonyl groups of the parent $[\text{Os}_3(\text{CO})_{10}(\mu\text{-H})_2]$. Ligand **I** in cluster **5** adopts the $\mu_3\text{-}1,2,4\text{-}\eta^3$ coordination mode. Like the parent cluster $[\text{Os}_3(\text{CO})_{10}(\mu\text{-H})_2]$,²⁹ one of the Os–Os distances (i.e. Os(4)–Os(5) = 2.6696(3) Å) is unusually short compared with the normal Os–Os single bond. We can tentatively assign the two spectroscopically detected hydrides to be bridging across the unusually short edge Os(4)–Os(5)

(28) Kabir, S. E.; Miah, A.; Nesa, L.; Uddin, K.; Hardcastle, K. L.; Rosenberg, E.; Deeming, A. J. *J. Organomet. Chem.* **1986**, *311*, 153.

(29) (a) Churchill, M. R.; Hollander, F. J.; Hutchinson, J. P. *Inorg. Chem.* **1977**, *16*, 2697. (b) Broach, R. W.; Williams, J. M. *Inorg. Chem.* **1979**, *18*, 314.

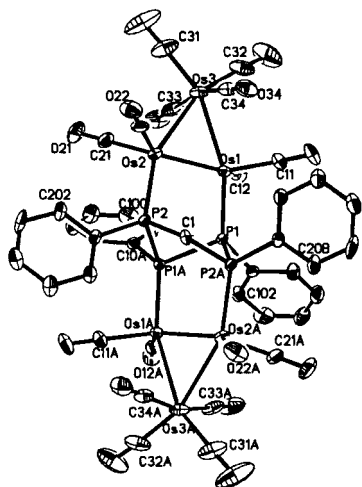


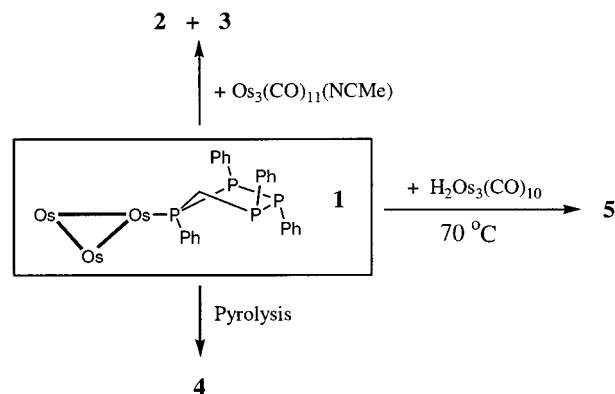
Figure 6. ORTEP drawing (thermal ellipsoid 30% probability) of cluster **6**.

(giving rise to some metal–metal double-bond character) on the basis of the electron count of 46 for the Os(4)Os(5)–Os(6) triosmium unit. The phenyl groups on the phosphorus atoms of the ligand moiety adopt an all-trans configuration. The P₄C ring of the ligand has the envelope configuration with C(1), P(1), P(3), and P(4) atoms almost coplanar (maximum deviation 0.022 Å), while P(2) is out of the above plane at a distance of 0.496 Å. The P(1)–P(2) distance (2.289(2) Å) is apparently longer than the other P–P bonds (average 2.232(2) Å) and than that in the free ligand (average 2.205 Å), which may be due to the coordination of both phosphorus atoms with heavy metals. The P(2)⋯P(4) distance (3.060 Å) is shortest among the nonbonding phosphorus–phosphorus distances; thus, we have assigned the large ²J_{PP} coupling constant (73.4 Hz) to be between these two phosphorus atoms. The P–Os bond distances are located in the typical range for such bonds.

The Cluster [$\{\text{Os}_3(\text{CO})_8(\mu\text{-H})_2\}_2\{\mu_4\text{-1,2,3,4-}\eta^4\text{-(PPh)}_4\text{-CH}_2\}$] (**6**). As also observed for cluster **2**, the ³¹P{¹H} NMR spectrum of cluster **6** shows an AA'XX' spin pattern. The ¹H NMR spectrum shows the existence of two sets of metal hydrides in the cluster with chemical shifts at –10.6 and –11.0 ppm, respectively.

The molecular structure of cluster **6** is given in Figure 6 together with the atomic labeling scheme, and the selected bond parameters are listed in Table 4. A crystallographic 2-fold axis passes through C(1) and the midpoint of the P(1)–P(1A) bond, resulting in the identical halves of the molecule. In the molecule, ligand **I** links each of the two different Os₃(CO)₈(μ-H)₂ units via one outer and one central phosphorus atom with the substitution of the carbonyl groups to adopt the μ₄-1,2,3,4-η⁴ coordination mode. Like cluster **5**, the Os(1)–Os(2) bond (2.6823(6) Å) has the properties of a double bond with two bridging hydrides, one above and the other below the osmium triangle plane. As in the free ligand, the phosphorus atoms in cluster **6** adopt the all-trans configuration. The P₄C ring has a twisted configuration with P(1) and P(1A) located symmetrically on opposite sides of the P(2)C(1)P(2A) plane at a distance of 0.13 Å. The average P–P bond length (2.262(2) Å) is elongated compared with

Scheme 3



that in the free ligand (2.205 Å) because of the coordination with heavy metal atoms.

Reactivity of the Monosubstituted Cluster [Os₃(CO)₁₁{(PPh)₄CH₂}] (**1**). Our experimental results demonstrate that the other three noncoordinated phosphorus atoms in cluster **1** can also participate in the coordination with metal atoms (Scheme 3). When cluster **1** reacts with an equimolar amount of the activated triosmium cluster [Os₃(CO)₁₁(NCMe)] at room temperature overnight, P(3) or P(4) can further coordinate to another cluster molecule and the 1,3- and 1,4-linked bis-trinuclear clusters **2** and **3** are obtained in 32% and 45% yields, respectively. When the solution of **1** in toluene is pyrolyzed at 100 °C for 4 h, the carbonyl groups in **1** are labilized and are displaced by the uncoordinated P(4) atom to give the disubstituted 1,4-bridged cluster **4**. When cluster **1** reacts with an equimolar amount of [Os₃(CO)₁₀(μ-H)₂] at 100 °C for 4 h in toluene, further coordination via P(2) and P(4) to another cluster molecule takes place to give the 1,2,4-linked bis-trinuclear cluster [Os₃(CO)₁₁{μ₃-1,2,4-η³-(PPh)₄CH₂}]{Os₃(CO)₈(μ-H)₂} (**5**).

Conclusions

Reactions of 1,2,3,4-tetraphenyl-1,2,3,4-tetraphospholane (**I**) with the activated triosmium cluster [Os₃(CO)₁₁(NCMe)] or [Os₃(CO)₁₀(μ-H)₂] under various conditions afford a series of trinuclear and linked bis-trinuclear clusters via the substitution of labile acetonitrile or carbonyl groups in parent clusters, wherein the ligand **I** shows a variety of coordination modes (η¹, μ-1,3-η², μ-1,4-η², μ₃-1,2,4-η³, μ₄-1,2,3,4-η⁴). Because of the coordination with metal atoms, the P–P bond(s) in the ligand moiety comprising the coordinated phosphorus are elongated compared with those of the free ligand. In cases where there are two M–P linkages, the extent of elongation of this bond is found to be even more pronounced. The magnitude of the ¹J_{PP} coupling constant is observed to be smaller, and again the extent of reduction is more significant when there are two M–P linkages. The existence of the red staggered conformer **1r** and the yellow eclipsed conformer **1y** in cluster **1** may stem from the intermolecular interactions in the crystalline state, while the two convertible configurational isomers (**3y** and **3r**) in the 1,3-linked bis-trinuclear cluster **3** arise due to the competition of the repulsion effect between the Ph⁴ on the uncoordinated

P(4) and the Os(CO)₄ unit with the repulsion among the phenyl groups attached on the intercylic phosphorus atoms. The ligand **I** is chiral at all coordinated phosphorus atoms, which results in the range of isomers obtained for some of the products. The high versatility of coordination modes in **I** may arise from the smaller cone angle of the two outer phosphorus atoms compared with other cyclopolyphosphines and the ready folding modes in the P₄C five-membered-ring, which preserves the ligand ring integrity after complexation.

Acknowledgment. We thank the National University of Singapore for financial support and for a Research Scholarship (to X.Z.).

Supporting Information Available: Complete listings of atomic positions, bond lengths and angles, anisotropic thermal parameters, hydrogen coordinates, data collection, and crystal parameters for all crystallographically characterized complexes. This material is available free of charge via the Internet at <http://pubs.acs.org>.

IC025589C